J Biomol NMR (2014) 60:275–281
DOI 10.1007/s10858-014-9869-4

NMR STRUCTURE NOTE

The B-box 1 dimer of human promyelocytic leukemia protein

Shu-Yu Huang · Mandar T. Naik · Chi-Fon Chang · Pei-Ju Fang · Ying-Hui Wang · Hsiu-Ming Shih · Tai-huang Huang

Received: 9 September 2014 / Accepted: 20 October 2014 / Published online: 30 October 2014

Biological context

SUMOylation, the enzyme-mediated reversible posttranslational modification by a small ubiquitin-like modifier (SUMO), is a crucial signalling event that regulates diverse cellular processes, including chromatin organization, transcription, DNA repair, macromolecular assembly, protein homeostasis, trafficking, and signal transduction (Flotho and Melchior 2013). Conjugating of SUMO to a substrate involves several steps. The matured SUMO is first activated and covalently linked to the SUMO E1 enzyme (SAE1–SAE2). In the second step SUMO is transferred to the SUMO E2-conjugating enzyme, Ubc9, which modifies the target substrate with the aid of a SUMO E3 ligase. Release of SUMO from target substrate is mediated by a SENP enzyme. Ubc9 usually modifies the lysine residue of substrate peptide in a consensus sequence, ΨKXD/E, where Ψ is a large hydrophobic residue and X is any residue. SUMO E3s confer substrate specificity and efficiency. Unlike ubiquitination where hundreds of E3 are known there are only few SUMO E3 ligases have been reported (Deshaies and Joazeiro 2009).

The promyelocytic leukemia protein (PML) (also known as TRIM19, MYL, RNF71 or PP8675) was first identified as the t(15; 17) chromosomal translocation partner of retinoic acid receptor-α (*RARa*) in acute promyelocytic leukemia (APL) (de The et al. 2012). The human *PML* gene can be alternatively spliced to generate multiple isoforms that have been classified into seven isoforms, PMLI-VII (Bernardi and Pandolfi 2007). All PML isoforms harbor the conserved N-terminal TRIM/RBCC motif containing three cysteine-rich zinc-binding domains, a RING (really interesting new gene) domain, two B-boxes (B-box 1 and B-box 2) and a coiled-coil region (CC) (Fig. 1a) but differ either in the central region or in the C-terminal region. PML is the major component and the key organizer of the PML

Electronic supplementary material The online version of this article (doi:10.1007/s10858-014-9869-4) contains supplementary material, which is available to authorized users.

S.-Y. Huang · M. T. Naik (✉) · P.-J. Fang · Y.-H. Wang · H.-M. Shih · T. Huang (✉)
Institute of Biomedical Sciences, Academia Sinica, Nankang, Taipei 11529, Taiwan, ROC
e-mail: n.mandar@gmail.com

T. Huang
e-mail: bmthh@ibms.sinica.edu.tw

S.-Y. Huang
Chemical Biology and Molecular Biophysics Program, Taiwan International Graduate Program, Institute of Biological Chemistry, Academia Sinica, Nankang, Taipei 11529, Taiwan, ROC

S.-Y. Huang
Institute of Biochemical Sciences, College of Life Science, National Taiwan University, Taipei 10617, Taiwan, ROC

Present Address:
M. T. Naik
Department of Biochemistry and Biophysics, Texas A&M University, 300 Olsen Boulevard, College Station, TX 77843-2128, USA

C.-F. Chang · T. Huang
Genomics Research Center, Academia Sinica, Nankang, Taipei 11529, Taiwan, ROC

T. Huang
Department of Physics, National Taiwan Normal University, Taipei 11677, Taiwan, ROC

Nuclear Bodies (PML NBs, also known as nuclear domain 10 (ND10), PODs and Kremer bodies) (Bernardi and Pandolfi 2007) which harbor more than 70 critical regulators and mediate significant activities. PML NBs are highly SUMOylated and their functions are strongly associated with SUMOylation process (Lallemand-Breitenbach et al. 2001). PML contains three SUMOylation sites (K65, K160 and K490). SUMOylation of K160 has been shown to be essential for PML's ability to recruit nuclear protein components to NBs. Using the tumor suppressor p53 and Mdm2 as substrates Chu et al. found that PML associated with Ubc9, p53 and Mdm2 and functions as a SUMO E3 ligase (Chu and Yang 2011). The E3 ligase activity of PML depended on intact structures of the RING and B-box domains. However, there is a paucity of detailed structural information for understanding the interactions. To provide structure insights of the mechanism of PML K160 SUMOylation and Ubc9/SUMO substrate interaction here we report the structure of the PML B-box 1.

Methods and results

Cloning, expression, and purification of recombinant proteins

The PML B-box 1 (residues 120–168) (Fig. 1b) was PCR amplified with flanking BamHI and XhoI restriction sites. The PCR products were then cloned into pGEX4T-1 vector (GE Healthcare) that contained an N-terminal GST tag followed by a thrombin cleavage site. The construct was transformed into BL21(DE3) and selected by ampicillin

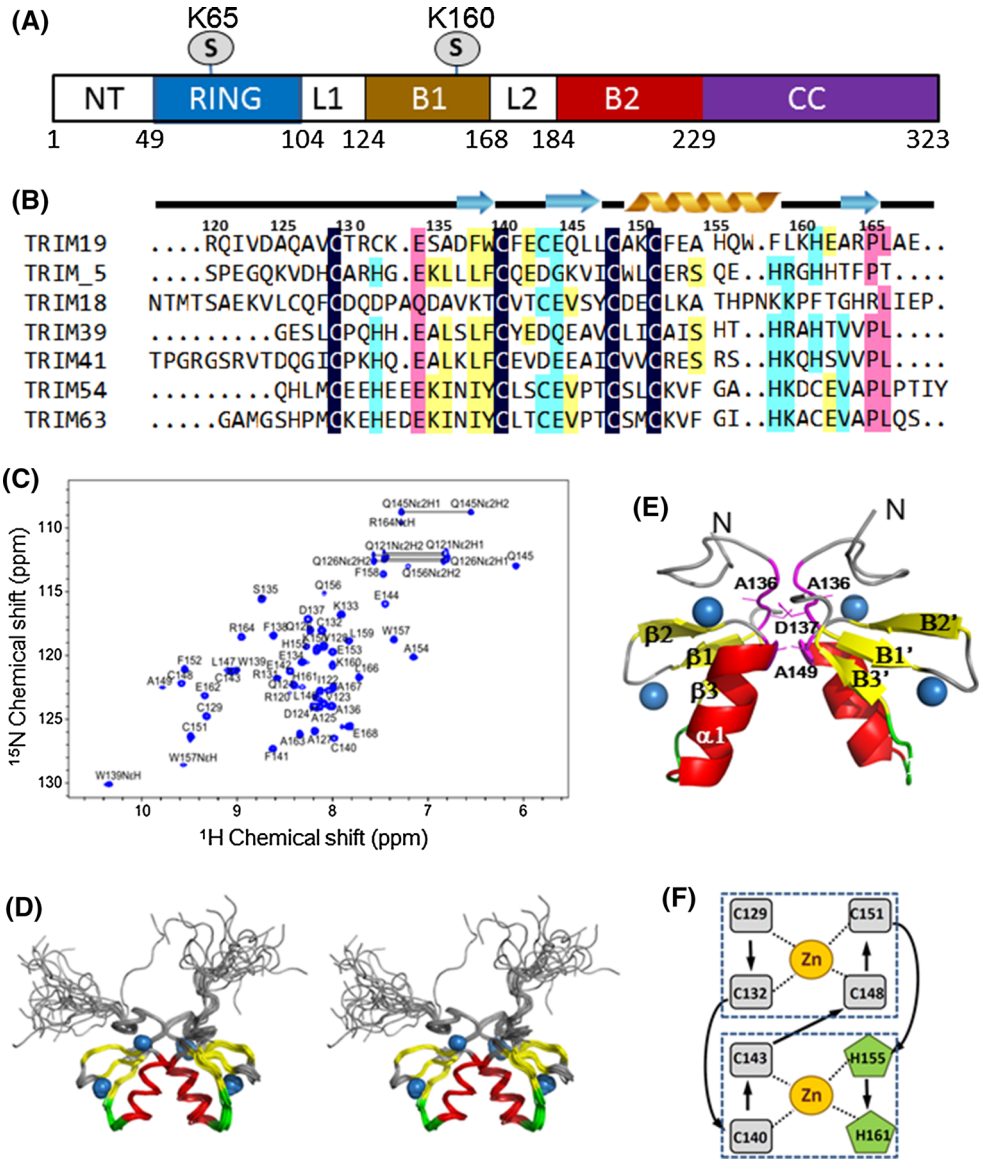

Fig. 1 **a** Domain organization of the PML TRIM motif. The *circled S* denotes the SUMOylation site. **b** Sequence alignment of the B-box 1 of human PML (TRIM19), TRIM5a, TRIM18 (MID1), TRIM39, TRIM41, TRIM54 and TRIM63 (MuRF1). The sequence number is that for the TRIM19 sequence. **c** ^{15}N-HSQC spectrum of PML B-box 1. **d** Stereo view of the overlay of backbone traces of 20 best PML B-box 1 dimer structures. The secondary features are color coded as follow: *grey* loop regions; *yellow* β strand; *red* α helix; *green* putative active site loop. The zinc ions are shown as *blue spheres*. **e** *Ribbon representation* of the structure of PML B-box 1 dimer. The unstructured N-terminal segment spanning residues Arg120–Gln126 are omitted. The secondary structure elements are labelled. The protomer interfacial residues are colored *magenta* and are labelled. **f** Schematic showing the cross-brace zinc-finger coordination of PML B-box 1

(Sigma). Clones were cultured in M9 minimal medium supplemented with 20 μm $ZnCl_2$ and incubated at 37 °C. Protein expression was induced at $OD_{600} \sim 0.8$ with 0.2 mM IPTG at 18 °C for overnight. Cells were harvested and lysed in buffer containing 50 mM Tris, 300 mM NaCl, 10 mM BME and 0.1 mM $ZnCl_2$ at pH 7.5. Expressed GST fusion proteins were purified through glutathione Sepharose 4B column (GE Healthcare), followed by size-exclusion chromatography (GE Superdex 75 16/40) in 25 mM Tris (pH 7.0), 100 mM NaCl, 1 mM $ZnCl_2$ and 0.2 mM Tris (2-carboxyethyl) phosphine (TCEP) (Sigma) buffer.

NMR spectroscopy

NMR spectra were acquired at 25 °C on a Bruker Avance 600 MHz NMR spectrometer equipped with 5 mm triple resonance cryoprobe and single axis pulsed field gradient. Samples for NMR experiments contain 1.0 mM protein in 25 mM Tris buffer (pH 7.0), 100 mM NaCl, 1 mM $ZnCl_2$ and 0.2 mM Tris (2-carboxyethyl) phosphine (TCEP) in 90 % (v/v) H_2O and 10 % (v/v) D_2O. Sequence specific assignments of backbone resonances were made from analysis of HNCA, HNCO, CBCANH, CBCA(CO)NH, and HNCACB spectra. Side chain resonances were assigned from analysis of the ^{15}N-edited NOESY-HSQC, ^{15}N-edited TOCSY-HSQC, H(CC)(CO)NH, (H)CC(CO)NH, (HB)CB(CGCD)HD, and (HB)CB(CGCDCE)HE spectra. ^{1}H chemical shifts were externally referenced to 0 ppm for methyl resonance of 2,2-dimthyl-2-silapentane-5-sulfonate (DSS), whereas ^{13}C and ^{15}N chemical shifts were indirectly referenced according to the IUPAC recommendations (Markley et al. 1998). NMR data were processed using software Topspin 2.0 and analyzed by software SPARKY (T. D. Goddard and D. G. Kneller, SPARKY 3, University of California, San Francisco, CS, USA). The ^{1}H, ^{15}N and ^{13}C resonances of the PML B-box 1 have been completely assigned (Fig. 1c) and the assignment data have been deposited in the BioMagResBank under accession numbers 25288.

NOE distance constrains were obtained from ^{15}N-edited NOESY-HSQC and ^{13}C-edited NOESY-HSQC spectra obtained at 150 ms mixing time. The aliphatic and aromatic ^{13}C-NOESYs were collected separately. The NOESY cross peaks were assigned automatically by CYANA and further checked manually. Since PML B-box 1 exists as a dimer we also acquired a ^{13}C-filtered, ^{15}N-edited 3D NOESY-HSQC spectrum at 100 ms mixing time and identified 43 inter-protomer NOEs (Zwahlen et al. 1997). Sample for the filter-edited experiment was prepared by mixing 1:1 molar ratio of unlabeled and ^{13}C, ^{15}N-labelled PML B-box 1 samples at 0.1 mM and further concentrated to 1.0 mM concentration. The backbone dihedral angle restrains, Φ and Ψ, were empirically predicted by the TALOS software program (Cornilescu et al. 1999). Pairwise hydrogen bond restraints were introduced for secondary structure elements predicted by CSI (Supplemental Figure S1) (Wishart and Sykes 1994). The presence of hydrogen bonds were further confirmed by hydrogen–deuterium exchange rates and NOEs. The structures were first calculated with CYANA v3.9 program (Guntert 2004) without hydrogen bond or zinc ion coordination restraints until the structures were well converged. Zinc ion coordination restraints reported in the MID1 B-box 1 structure were employed (Massiah et al. 2007). Introduction of the zinc ions did not produce additional NOE violation. Families of structures were further refined using software XPLOR-NIH v.2.36 (Schwieters et al. 2003). The structure quality was checked by analyzing the NOE and geometric deviations of the calculated conformers using MolMol (Koradi et al. 1996) and Procheck (Laskowski et al. 1996) software programs. The structure coordinates have been deposited (PDB ID code 2mvw).

The ^{15}N-R_1, ^{15}N-R_2, and [^{1}H–^{15}N]NOE were determined as previously described (Kay et al. 1992). Each ^{15}N-R_1 was determined with delays of 0, 90, 190, 310, 460, 650, 930, and 1,500 ms in random order. Similarly, each ^{15}N-R_2 was determined from randomly ordered delays of 0, 17, 34, 68, 119, 170, 237, and 339 ms. The rate constants were determined from peak intensities using the program Protein Dynamics Center (Bruker, Germany). The errors in peak intensities were calculated from two duplicate experiments. The steady-state heteronuclear [^{1}H–^{15}N] NOE experiment was carried out in duplicate in an interleaved manner, with and without proton saturation. The NOEs were calculated as the error-weighted average ratio of peak intensities, with error estimated by standard deviation of three pairs of repeated experiments. The reduced spectral density analysis was performed as previously described (Farrow et al. 1995; Lefevre et al. 1996).

Overview of the B-box 1 structure

The ^{1}H–^{15}N heteronuclear single quantum coherence (HSQC) spectrum of B-box 1 spanning residues 120–168 at 1.0 mM concentration was well-dispersed (Fig. 1c). Analytical ultracentrifugation (AUC) results and rotational correlation time determined from NMR (To be discussed later) showed that the protein exists as a dimer at this concentration. The solution structure of the dimeric PML B-box 1 was computed based on empirical NMR restraints containing 1,391 NOE restraints (785 sequential, 213 medium range, 393 long range intramolecular and 43 intermolecular), 27 hydrogen bond restraints, and 84 dihedral angle restraints. An overlay of the backbone traces of 20 best structures is shown on Fig. 1d and a summary of the structure statistics is given in Table 1. The root-mean-

Table 1 NMR structure calculation and refinement statistics for PML B-box 1 protein

NMR distance and dihedral constraints	
Distance constraints	
Total NOE	1,391
Sequential ($\|i-j\|=1$)	785
Medium-range ($1<\|i-j\|<5$)	213
Long-range ($\|i-j\|\geqq 5$)	393
Intermolecular	43
Hydrogen bonds	27
Total dihedral angle restraints	
ϕ	42
ψ	42
Average pairwise RMSD (Å)[a]	
Backbone	0.36
Heavy atom	0.82
Ramachandran plot[b]	
Residues in most favorable regions (%)	82.7
Residues in additional favorable regions (%)	15.7
Residues in generously favorable regions (%)	1.6
Residues in disallowed regions (%)	0.0

[a] RMSD of the Xplor-NIH refined ensemble of 20 structures with the lowest energy, selected from 64 calculated structures. The RMSD was calculated for the structured regions of B-box 1 monomer consisting of residues 127–167 and 227–267

[b] The Ramachandran plot was generated by PROCHECK for the 20 lowest energy structures included in RMSD calculation

square-deviation (RMSD) for the structured region containing residues 127–167 is 0.36 Å for the backbone atoms and 0.82 Å for all heavy atoms. The Ramachandran plot analysis indicated that 82.7 % of residues are in the most favored region, 15.7 % in the additionally allowed region, 1.6 % in the generously allowed region and none in the disallowed region.

The solution structure of PML B-box 1 is a butterfly-shaped homodimer with the two protomers contacting each other on one end of the structure at an angle of ~40° (Fig. 1d, e). Each protomer comprises a three-stranded anti-parallel β-sheets (β1, 138–140; β2, 144–147; β3, 163–165) and one helix (α1, 149–158) in a ββαβ topology. The N-terminal segment spanning residues Ser120 to Ala125 is disordered. The two protomers are held together through mostly hydrophobic interactions between residues Ser135–Asp137 and Ala149 on one protomer to the counterparts on the other protomer (Fig. 1e). The distance between backbone Cα of Asp137 on one protomer and Cα of Lys150 on the other protomer is 6.4 Å, thus the side chains of these two residues potentially can form a salt bridge. The protein contains two cross-brace zinc-finger domains with Cys129, Cys132, Cys148, and Cys151 together constituting the first C4-type zinc-finger domain and Cys140, Cys143, His155, and His161 forming the second C2H2-type zinc-finger domain (Fig. 1f). The presence of two zinc ions per B-box 1 molecule was confirmed by inductively coupled plasma mass spectrometry mass (ICP-mass) (Data not shown).

Dynamics of PML B-box 1

The dynamics of PML B1 was investigated by reduced spectral density function analysis calculated from backbone amide ^{15}N relaxation parameters (Fig. 2b). The results showed that the central region of PML B-box 1 spanning residues Ala127–Ala167 is well-ordered with average [^{1}H–^{15}N]-NOE of ~0.76 and small J(ω_H), suggesting the presence of little picosecond fast motion. However, J(0) of residues Cys129, Cys132, Leu146 and Ala149 in the first zinc-finger domain, and Leu159 and His161 in the second zinc-finger domain are considerably larger than the average, indicating the presence of considerable slow local motion in the zinc-finger domains. Interestingly, the segment spanning residues Ile122 to Gln126 near the N-terminus showed a slow decreasing non-vanishing NOE, suggesting the presence of residual structure. The functional roles of the local motion are yet to be explored.

The presence of zinc ion is absolutely essential for the structural integrity of PML B-box 1. To test the effect of destroy a zinc-finger on the overall structure of PML B-box 1 we mutated histidine 161 to alanine and acquired ^{15}NH relaxation parameters for backbone amide ^{15}N. The mutant protein contains only one zinc ion, as verified by ICP-Mass. The ^{15}N-HSQC spectrum of the u-^{15}N-H161A mutant showed that protein is still largely structured and the backbone resonances have been fully assigned (data not shown). The considerable structural integrity was supported by the retention of near intact [^{1}H–^{15}N]-NOE for majority of the resonances (red dots in Fig. 2a). As expected, the second zinc-finger site was disordered as shown by the negative values of [^{1}H–^{15}N]-NOE for residues Cys143 and the segment spanning residues Phe158–Leu166. Surprisingly, eliminating the second zing-finger domain also affected the dynamics of the first one as shown by the significant drop in [^{1}H–^{15}N]-NOEs for residues Val128 and Asp137.

Discussion and conclusion

PML is a member of the tripartite motif family of proteins (TRIM/RBCC) which consists of ~70 members in humans and mice (Meroni 2012). TRIM proteins are characterized by the presence of the N-terminal tripartite motif and a variable C-terminal region that may contain various

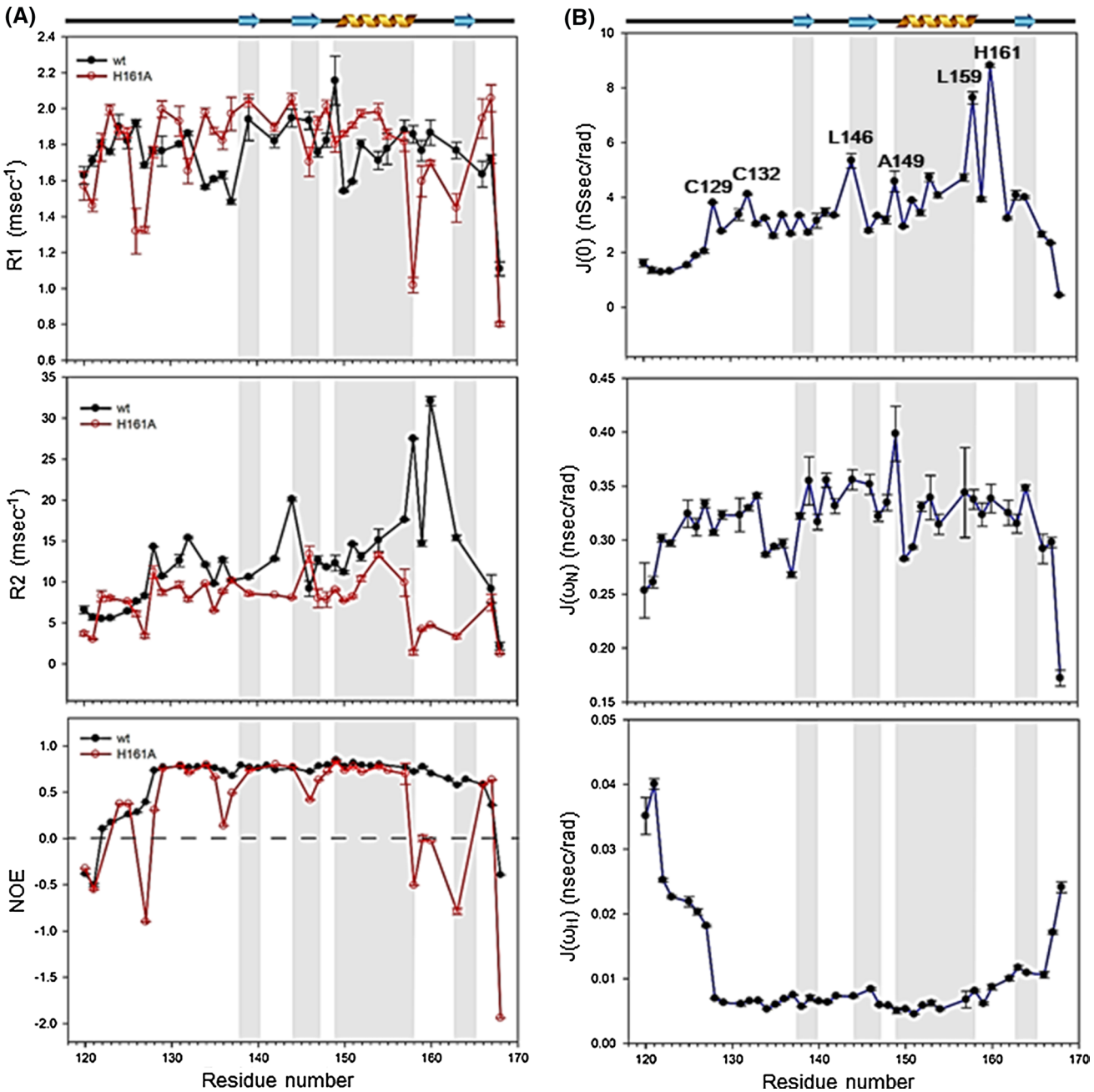

Fig. 2 Dynamics of PML B-box 1. **a** ^{15}N-R1 (*top panel*), ^{15}N-R2 (*middle panel*) and [^{1}H–^{15}N]-NOE (*bottom panel*) data of PML B-box 1 (*black*) and PML B-box 1 H161A mutant (*red*). **b** Reduced spectral density functions, J(0) (*top panel*), J(ω_N) (*middle panel*), J(ω_H) (*bottom panel*) deduced from relaxation data shown on **a**

domains. These proteins have been implicated in diverse cellular processes, including apoptosis, transcriptional regulation, oncogenesis, innate immune response, cellular development and muscle physiology. More recently, it was suggested that some TRIM proteins such as PML, RFP and TRIM32 may be a new class of SUMO protein E3 ligases (SUMO E3) and their SUMO activity depending on an intact tripartite motif (Chu and Yang 2011). Due to the large number of substrates that can be targeted by an E3 ligase, mutations in *RBCC/TRIM* genes can result in several pathological conditions (Cammas et al. 2012). The structure reported here provide a starting point for understand the structural basis of the function of TRIM proteins. Comparison of the structure of PML B-box 1 to known B-box 1 structures showed a RMSD of 1.260 and 1.863 Å for human MID1 (TRIM18, pdb ID: 2FFW) and TRIM39 (pdb ID: 2DIF), respectively (Fig. 3a). Thus, the structures of the three B-box 1 domains are highly homologous.

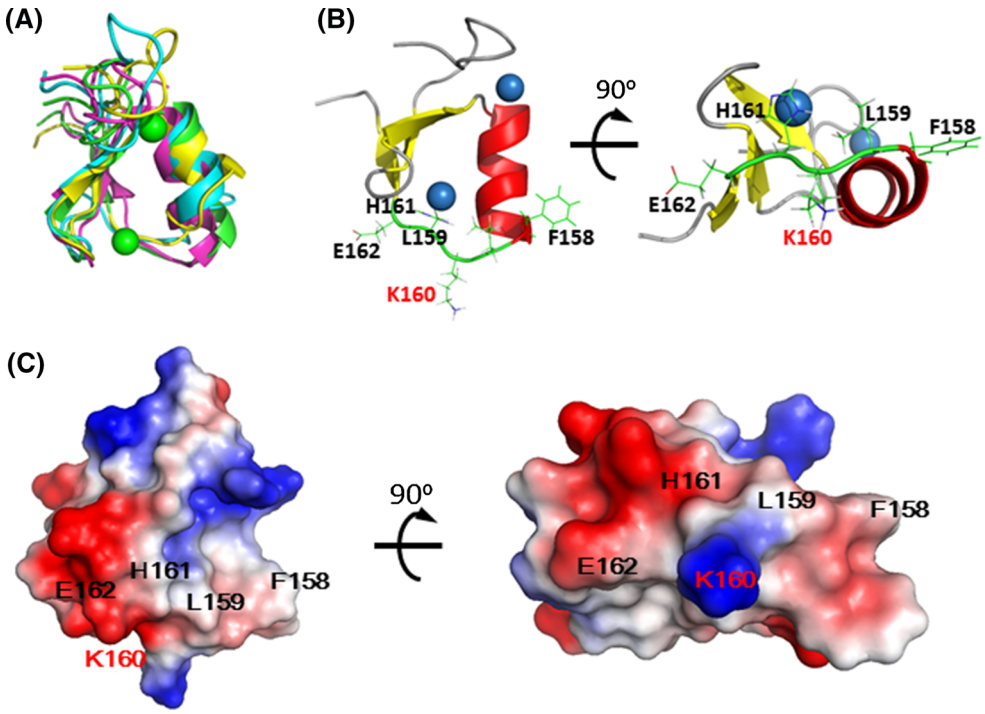

Fig. 3 **a** Comparison of PML B-box 1 protomer structure with homologous B-box domains. *Green* PML B-box 1 protomer; *cyan* human MID1 B-box 1 (PDB ID: 2FFW); *magenta* TRIM39 B-box 1 (PDB ID: 2DIF); *yellow* human MID1 B-box 2 (PDB ID: 2DQ5). The *two green spheres* are zinc ions coordinated to PML B-box 1 protomer. **b** Spatial arrangements of the acceptor site residues of PML B-box 1. *Left* side view; *right* bottom view. Side chains of residues likely to interact with Ubc9 are shown in *lines*. The acceptor residue, K160, was labelled *red*. **b** Surface charge distribution of PML B-box 1 shown in the same orientations as in **b**

When compared to the structure of B-box 2 from human MID1 (pdb ID: 2DQ5)) the RMSD was 1.094 Å, suggesting that the structures of PML B-box 1 and MID1 B-box 2 are also rather similar as well.

PML itself is also a SUMO substrate containing three SUMOylation sites (Flotho and Melchior 2013). The SUMOylation of K160 is particularly important for its role in forming the PML NBs. We found that the PML B-box 1 SUMOylation motif, ΨKXE/D, exists as an extended loop located at one end of the structure with the SUMO acceptor K160 sitting at the tip of the loop (Fig. 3b). We can envision the loop to be inserted into the active site cleft of Ubc9 SUMO E2 conjugating enzyme ready for SUMOylation. The surface charge distribution of the PML B-box 1 further showed that K160 is sandwich between a large patch of the hydrophobic residues consisting of Phe158 and Leu159 on one side and a negatively charged patch consisting of residues Glu142, Glu144 and Glu162 on the other side (Fig. 3c). The charge distribution complements that around the active site of Ubc9 where the active side Cys93 residue was juxtaposed between a hydrophobic surface formed by Val86, Tyr87 and Tyr134 on one side and a large positively charged surface formed by Lys59, Lys65, Lys74 and Lys76 on the other side. Similar binding mode has been proposed for the recognition of a SUMO substrate, RanGAP, and Ubc9 (pdb ID: 2GRN) (Bernier-Villamor et al. 2002). We are in the process of performing a more detailed characterization of the interaction between PML B-box 1 and Ubc9. Preliminary results confirmed our proposed interaction mechanism and a more detailed description of the results will be published in the future. Spectral density analysis revealed that residues Leu159 and His161 exhibit considerable slow motion as characterized by their large J(0) values. These two residues are in between of the active site residue, Lys160, indicating that the SUMOylation motif is undergoing slow motion. The flexibility of the loop should be favorable for optimizing the interactions with Ubc9's catalytic site residues and facilitates SUMO transfer. We are in the process of determining the structure of PML B-box 1/Ubc9 complex for elucidating the detailed interaction between them and also exploring the possible role of loop dynamics in SUMO transfer.

The rotational correlation time, τ_c, can be calculated from the ratio of the spectral density functions, $\tau_c^2 = \omega_N^2[J(0) - J(\omega_N)]/J(\omega_N)$, of rigid backbone amide ^{15}N sites (Lefevre et al. 1996). We obtained a value of 7.5 ns for PML B-box 1. This correlation time is too long for a monomeric PML B-box 1 and is closer to that expected for a dimer. This prompted us to conduct an analytical ultracentrifugation (AUC) study of the oligomerization state of PML B-box 1. Preliminary results showed that the protein exists as a monomer at 6 μM concentration and under our NMR experimental condition of 1 mM the protein is indeed a dimer. Thus, the structure we determined is a dimer. We are conducting more thorough studies to gain quantitative understandings of the oligomerization behavior of PML B-box 1 and its functional implications.

Acknowledgments The NMR experiments were conducted on NMR spectrometers at the High-Field Nuclear Magnetic Resonance Center (HFNMRC), supported by the National Research Program for Biopharmaceuticals, the Ministry of Science and Technology Republic of China. This work was supported by a grant from the Ministry of Science and Technology, Republic of China to T.H.H. (NSC102-2113-M-001-010).

References

Bernardi R, Pandolfi PP (2007) Structure, dynamics and functions of promyelocytic leukaemia nuclear bodies. Nat Rev Mol Cell Biol 8:1006–1016

Bernier-Villamor V, Sampson DA, Matunis MJ, Lima CD (2002) Structural basis for E2-mediated SUMO conjugation revealed by a complex between ubiquitin-conjugating enzyme Ubc9 and RanGAP1. Cell 108:345–356

Cammas F, Khetchoumian K, Chambon P, Losson R (2012) Trim involvement in transcriptional regulation. Trim Rbcc Proteins 770:59–76

Chu Y, Yang X (2011) SUMO E3 ligase activity of TRIM proteins. Oncogene 30:1108–1116

Cornilescu G, Delaglio F, Bax A (1999) Protein backbone angle restraints from searching a database for chemical shift and sequence homology. J Biomol NMR 13:289–302

de The H, Le Bras M, Lallemand-Breitenbach V (2012) The cell biology of disease: acute promyelocytic leukemia, arsenic, and PML bodies. J Cell Biol 198:11–21

Deshaies RJ, Joazeiro CA (2009) RING domain E3 ubiquitin ligases. Annu Rev Biochem 78:399–434

Farrow NA, Zhang O, Szabo A, Torchia DA, Kay LE (1995) Spectral Density mapping using 15N relaxation data exclusively. J Biomol NMR 6:153–162

Flotho A, Melchior F (2013) Sumoylation: a regulatory protein modification in health and disease. Annu Rev Biochem 82:357–385

Guntert P (2004) Automated NMR structure calculation with CYANA. Methods Mol Biol 278:353–378

Kay LE, Nicholson L, Delaglio F, Bax A, Torchia D (1992) Pulse sequences for removal of the effects of cross correlation between dipolar and chemical-shift anisotropy relaxation mechanisms on the measurement of heteronuclear T1 and T2 values in proteins. J Magn Reson 97:39–375

Koradi R, Billeter M, Wuthrich K (1996) MOLMOL: a program for display and analysis of macromolecular structures. J Mol Gr 14:51–55

Lallemand-Breitenbach V, Zhu J, Puvion F, Koken M, Honore N, Doubeikovsky E, Duprez E, Pandol PP, Puvion E, Freemont PS, de The H (2001) Role of promyelocytic leukemia (Pml) sumolation in nuclear body formation, 11s proteasome recruitment, and as2O3-induced Pml or Pml/retinoic acid receptor α degradation. J Exp Med 193:1361–1371

Laskowski RA, Rullmann JAC, MacArthur MW, Kaptein R, Thornton JM (1996) AQUA and PROCHECK—NMR: programs for checking the quality of protein structures solved by NMR. J Biomol NMR 8:477–486

Lefevre JF, Dayie KT, Peng JW, Wagner G (1996) Internal mobility in the partially folded DNA binding and dimerization domains of GAL4: NMR analysis of the N–H spectral density functions. Biochemistry 35:2674–2686

Markley JL, Bax A, Arata Y, Hilbers CW, Kaptein R, Sykes BD, Wright PE, Wuthrich K (1998) Recommendations for the presentation of NMR structures of proteins and nucleic acids. IUPAC-IUBMB-IUPAB inter-union task group on the standardization of data bases of protein and nucleic acid structures determined by NMR spectroscopy. J Biomol NMR 12:1–23

Massiah MA, Matts JAB, Short KM, Simmons BN, Singireddy S, Yi Z, Cox TC (2007) Solution structure of the MID1 B-box2 CHC(D/C)C2H2 zinc-binding domain: insights into an evolutionarily conserved RING fold. J Mol Biol 369:1–10

Meroni G (2012) Genomics and evolution of the TRIM gene family. Adv Exp Med Biol 770:1–9

Schwieters CD, Kuszewski JJ, Tjandra N, Clore GM (2003) The Xplor-NIH NMR molecular structure determination package. J Magn Reson 160:65–73

Wishart DS, Sykes BD (1994) Chemical shifts as a tool for structure determination. Methods Enzymol 239:363–392

Zwahlen C, Legault P, Vincent SJF, Greenblatt J, Konrat R, Kay LE (1997) Methods for measurement of intermolecular NOEs by multinuclear NMR spectroscopy: application to a bacteriophage lamda N-peptide/boxB RNA complex. J Am Chem Soc 119:6711–6721